Nigerian Journal of Physics (NJP)
ISSN online: 3027-0936
ISSN print: 1595-0611
DOI: https://doi.org/10.62292/njp.v35i2.2026.570
Volume 35(2), June 2026

Computational Evaluation of Gamma-Ray Shielding and Photon Interaction Parameters of Bi_2O_3-Modified Tm^{3+}-Doped Borotellurite Glasses using Phy-X/PSD

*[1,2]Ibrahim Maijawa, [2]Usman Muhammad Ibrahim, [3]Musa Muhammad Elbulatory, [4]Mala Bukar and [4]Dauda Aminu Idiss

[1]Department of Physics, Federal University Gashua, Yobe State, Nigeria.
[2]Department of Physics, Bayero University Kano, Kano State, Nigeria.
[3]Department of Physics, Yobe State University, Damaturu, Yobe State, Nigeria.
[4]Zonal Advanced Space Technology Application Laboratory, under National Space Research and Development Agency, Kano State, Nigeria.

*Corresponding Author's Email: ibraheemmaijawa@gmail.com Phone: +2348108127253

ABSTRACT

The demand for efficient, transparent, and environmentally friendly radiation shielding materials has intensified with the increasing use of ionizing radiation in medical, industrial, and nuclear applications. In this study, the gamma-ray shielding and photon interaction characteristics of Bi_2O_3-modified Tm^{3+}-doped borotellurite glasses were systematically evaluated using the Phy-X/PSD computational platform. Five glass compositions with varying Bi_2O_3 content (0–0.20 mol %) were analyzed over a broad photon energy range of 0.015–15 MeV to investigate the influence of bismuth oxide incorporation on shielding performance. Key photon interaction parameters, including effective atomic number (Z_{eff}), effective electron density (N_{eff}), and effective conductivity (C_{eff}), were calculated at energies corresponding to commonly used gamma-ray sources (Am-241, Cs-137, and Co-60). The density of the glass samples was found to increase gradually from 5.106 to 7.203 g/cm^3 with the Bi_2O_3 addition (0–0.2 mol %). The results reveal a pronounced enhancement in radiation attenuation capability with increasing Bi_2O_3 concentration, primarily due to the high atomic number and density of bismuth oxide. Z_{eff} exhibited a consistent increase across all photon energies, indicating improved photon interaction probability. N_{eff} showed strong energy dependence, decreasing at low photon energy where photoelectric absorption dominates, while increasing at intermediate and high energies due to enhanced Compton scattering. Similarly, C_{eff} attained maximum values at low photon energy and decreased gradually with increasing energy, reflecting transitions between dominant photon interaction mechanisms. Among the investigated compositions, the glass containing 0.20 mol % Bi_2O_3 demonstrated the best overall shielding performance across the entire energy range. These findings confirm that Bi_2O_3-modified borotellurite glasses are promising transparent, lead-free candidates for advanced gamma-ray shielding applications in medical imaging facilities, nuclear laboratories, and radiation protection systems.

Keywords:
Bi_2O_3-modified glass,
Borotellurite glass,
Gamma-ray shielding,
Lead-free shielding materials,
Photon interaction parameters,
Phy-X/PSD.

INTRODUCTION

The fundamental purpose of radiation shielding is to limit, control, or modify the radiation exposure rate at a specific point. Shielding is based on attenuation, the gradual reduction in the intensity of energy as it passes through a medium. Without adequate shielding, individuals could be exposed to radiation levels exceeding regulated limits, potentially leading to negative health effects. While complete avoidance of radiation exposure is often impossible, effective shielding is a critical consideration in any environment where radiation sources are present (Hussain *et al*., 2022). The principle of As Low As Reasonably Achievable (ALARA) guides radiation protection efforts,

emphasizing the importance of minimizing exposure while acknowledging the beneficial uses of radiation (Frane & Bitterman, 2025).

The performance as a radiation shielding material is determined mainly by its density, atomic number and chemical composition of the material. In general, denser material is better (more attenuating) since there are more atoms per unit volume to interact with the radiation (Yin *et al*., 2022). Materials with high atomic numbers enhance the attenuation of gamma rays and X-rays by the enhanced likelihood of photoelectric absorption and pair production (Alomari, 2024).

Effective radiation shielding relies on utilizing materials that can effectively reduce the strength of ionizing radiation. Over the years, many materials have been used, all with their own advantages and disadvantages. Most recently, material science has progressed into creating new shielding materials with custom designs and properties.

Lead was the primary material used for radiation shielding for many years due to its high density (11.34 g/cm^3) and high atomic number (Z is 82) (Wang *et al*., 2020). Lead is widely used in medical imaging rooms, nuclear facilities, and other industrial applications as sheets, bricks, Personal Protective Equipment (PPE), and a variety of other products. However, handling and disposing of the equipment might be challenging due to lead's toxicity and weight (Bawazeer *et al*., 2023; Naja & Volesky, 2017; Raj & Das, 2023).

Another traditional construction material which is widely used for radiation shielding is concrete. This is particularly applicable in large scale structures such as nuclear power plants or medical radiotherapy rooms (Hussain *et al*., 2022). Due to it being cost efficient and having the ability to provide protection from gamma rays and neutrons, it is used in versatile settings. Incorporation of high density aggregates such as barite or magnetite also allow for improvement of concrete's structural effectiveness. Using boron compounds can enhance concrete's effectiveness to absorb neutrons. Concrete is dense, which makes it crack prone over long periods of time (Barbhuiya *et al*., 2025; Munakata *et al*., 2009).

Among emerging radiation shielding materials, glasses and composites are receiving increasing interest in recent years. Hence, glasses have an advantage of transparency which is important for visual observation required by medical imaging and nuclear hot cells (AbuAlRoos *et al*., 2019).

Borotellurite glasses have high average refractive index typically greater than 1.8. This large refractive index will be useful in many light devices and may increase the probability of their interaction with radiation. Moreover, these glasses possess a broad transmission window ranging from visible to mid-infrared part of the electromagnetic spectrum (Kaur *et al*., 2016). This transparency is an important benefit for radiation shielding applications in which one must be able to visually inspect the shielded region, such as medical and nuclear environments. These may be enhanced by incorporating heavy metal oxides, such as PbO or Bi_2O_3, in the glassy phase (Kaur *et al*., 2016). Light weight and flexible shielding materials can be created by adding the high-z nanoparticles into glass composites, which can find application in medical fields to substitute lead (Marzuki *et al*., 2025).

The incorporation of Bi_2O_3, which has a high density (8.9 g/cm^3) and atomic number (Z is 83), generally leads to an increase in the density of the glass matrix (Kaur *et al*., 2016). This increase in density is a crucial factor for enhancing the radiation shielding effectiveness of the glass, particularly against gamma rays and X-rays, as it increases the probability of interaction between the radiation and the material (Azuraida *et al*., 2022). The refractive index of the glass also tends to increase with the addition of Bi_2O_3, which can be beneficial for optical applications (Ibrahim *et al*., 2024).

Several studies have investigated radiation shielding properties of heavy metal oxide glasses using both experimental and computational approaches. Sayyed *et al*., (2020) used a combination of theoretical and simulation code methodologies, to study the radiation shielding efficacy of $(40 + x)PbO - 5TeO_2 - 15BaO - (20 - x)Na_2O - 20B_2O_3$ glasses, where x represented PbO concentrations of 0, 5, 10, 15, and 20 mol %. The authors reported that the Mass Attenuation Coefficients (MACs) of the synthesized glasses were directly proportional to the lead oxide (PbO) concentration, indicating enhanced shielding with higher PbO content. Conversely, the MACs were observed to diminish with increasing incident photon energy. Alothman *et al*., (2021) analyzed the impact of molybdenum trioxide (MoO_3) on the radiation shielding capabilities of $55B_2O_3 - 30Pb_3O_4 - (15 - x)Al_2O_3 - xMoO_3$ glasses, where MoO_3 content (x) was incrementally varied from 0 to 5 mol %. The investigation demonstrated that the glass composition with the highest MoO_3 concentration yielded the most effective attenuation for both photons and fast neutrons. However, PbO's inherent toxicity presents an environmental drawback. Additionally, lead's opaque nature restricts its use in modern facilities that require transparent shielding. Despite these advances, limited attention has been given to the energy-dependent behavior of advanced photon interaction parameters, including effective atomic number (Z_{eff}), effective electron density (N_{eff}), and effective conductivity (C_{eff}), particularly in Bi_2O_3-modified rare-earth-doped borotellurite glass systems. Moreover, the combined influence of Bi_2O_3 concentration and Tm^{3+} doping on photon interaction mechanisms over a broad energy spectrum remains insufficiently explored. In this work, a comprehensive computational evaluation of gamma-ray shielding and

photon interaction parameters of Bi_2O_3-modified Tm^{3+}-doped borotellurite glasses is presented using the Phy-X/PSD simulation platform. Unlike previous studies, this research systematically investigates the energy-dependent variation of Z_{eff}, N_{eff}, and C_{eff} across a wide photon energy range (0.015–15 MeV) for multiple Bi_2O_3 concentrations. The study provides new insights into the dominant photon interaction mechanisms governing attenuation behavior in heavy metal oxide glasses and highlights the potential of Bi_2O_3-doped borotellurite glasses as environmentally friendly, transparent, lead-free radiation shielding materials for medical and nuclear applications.

MATERIALS AND METHODS

Theoretical Background

The interaction of gamma photons with matter depends strongly on the atomic composition, density, and electronic structure of the shielding material. To evaluate the radiation shielding capability of the investigated glass samples, several photon interaction parameters were calculated, including the Effective Atomic Number (Z_{eff}), Effective Electron Density (N_{eff}), and Effective Conductivity (C_{eff}). These parameters provide important insight into the mechanisms governing photon attenuation within the glass matrix.

Effective Atomic Number (Z_{eff})

The effective atomic number represents the equivalent atomic number of a composite material that characterizes its interaction with photons. For multi-element materials such as glasses, Z_{eff} is used to describe the overall contribution of different constituent elements in photon–matter interactions. It is particularly useful for understanding gamma-ray attenuation since different interaction processes (photoelectric absorption, Compton scattering, and pair production) depend on the atomic number of the absorbing medium. The effective atomic number of a material can be calculated from the ratio of the total atomic cross section (σ_a) to the total electronic cross section (σ_e) using the following relation as mentioned by Şakar *et al*., (2020):

$$Z_{eff} = \frac{\delta a}{\delta e} \quad (1)$$

$$\sigma_a = \frac{N\mu_m}{NA} \quad (2)$$

$$\sigma_e = \frac{1}{NA}\left(\sum_i \frac{F_i A_i}{Z_i}(\mu_m)_i\right) = \frac{\sigma_a}{Z_{eff}} \quad (3)$$

where σ_a (cm^2/g) is the total atomic cross section; σ_e (cm^2/g) is the total electronic cross section; N_A is the Avogadro number; $F_i, A_i and\ Z_i$ are the mole fraction, atomic weight, and atomic number of the *ith* involved element, respectively.

The effective atomic number is an important parameter because materials with higher Z_{eff} generally exhibit stronger photon attenuation, particularly at low photon energies where the photoelectric absorption process dominates.

Effective Electron Density (N_{eff})

The effective electron density describes the number of electrons available per unit mass of a material that can participate in photon interactions. It is particularly relevant in the Compton scattering region, where photon interactions depend mainly on electron density rather than atomic number. The effective electron density can be expressed by the following relation as mentioned by Şakar *et al*., (2020):

$$N_{eff} = \frac{N_A}{N} Z_{eff} \sum_i n_i = \frac{\mu_m}{\sigma_e} \quad (4)$$

where σ_a (cm^2/g) is the total atomic cross section; σ_e (cm^2/g) is the total electronic cross section; N_A is the Avogadro number; $F_i, A_i and\ Z_i$ are the mole fraction, atomic weight, and atomic number of the *ith* involved element, respectively.

Higher electron density indicates a larger number of available electrons for photon interactions, which contributes to enhanced radiation attenuation properties.

Effective Conductivity (C_{eff})

Effective conductivity is another parameter related to the interaction of photons with electrons in the material. It represents the ability of the material to respond to electromagnetic interactions caused by incident radiation. The effective conductivity (C_{eff}; in S/m) can be calculated according to the next expression mentioned by Kamislioglu, (2021):

$$C_{eff} = \left(\frac{N_{eff}\rho e^2 \tau}{m_e}\right) 10^3 \quad (5)$$

where e(C) and m_e (Kg) are the charge and mass of the electron respectively, $\tau(s)$ is the average life time (relaxation time) of the electron at the Fermi surface and is defined by the following formula (Devillers, 1984 and Şakar *et al*., 2020):

$$\tau = \frac{\hbar}{K_B T} = \frac{h}{2\pi K_B T} \quad (6)$$

where h (j.s) and K_B (J/K) are the Planck and Boltzman Constant, T (K) is the temperature of the environment.

Glass Composition

In this study, the radiation shielding characteristics of Bi_2O_3-modified thulium-doped borotellurite glasses were investigated through computational analysis. The glass system considered has the general composition: $B_2O_{3(0.59-y)} - TeO_{2(0.3)} - Bi_2O_{3(y)} - LiF_{(0.1)}: Tm_2O_{3(0.01)}$ where y=0, 0.05, 0.1, 0.15, and 0.2 mol %. The variation in the Bi_2O_3 concentration was introduced to examine its influence on the photon attenuation capability of the glass matrix. Five different glass samples were considered and labeled S1–S5 depending on the amount of Bi_2O_3 incorporated. The densities of the investigated glass samples range from

5.106 g/cm³ to 7.203 g/cm³, increasing with the concentration of Bi_2O_3 due to the high atomic mass of bismuth oxide. The detailed chemical compositions and densities of the studied glasses are presented in Table 1.

Table 1: The Sample Code, Chemical Formula, Concentration of Materials, and Densities of the Glass Samples

Glass Code	Glass Composition					Density (g/cm³)
	Concentration of the Materials (mol %)					
	B_2O_3	TeO_2	Bi_2O_3	LiF	Tm_2O_3	
S1	0.59	0.30	0.00	0.10	0.01	5.106
S2	0.54	0.30	0.05	0.10	0.01	5.910
S3	0.49	0.30	0.10	0.10	0.01	6.301
S4	0.44	0.30	0.15	0.10	0.01	6.820
S5	0.39	0.30	0.20	0.10	0.01	7.203

(Laxmikanth et al., 2025)

Computational Method

The radiation shielding parameters of the investigated glasses were evaluated using the online simulation platform Phy-X/PSD, which was developed for calculating photon interaction and radiation shielding parameters of composite materials. This software enables the determination of various attenuation and interaction parameters based on the chemical composition and density of the material. Initially, the chemical compositions of the glass samples in mol % and their corresponding densities (g/cm³) were entered into the simulation interface of the Phy-X/PSD platform. The calculations were performed over a wide photon energy range of 0.015–15 MeV using the "Standard Grid" energy option, which allows for a comprehensive analysis of energy-dependent photon interactions. To simulate realistic radiation environments, photon energies corresponding to commonly used gamma-ray sources were selected, including: Americium-241 (0.060 MeV), Cesium-137 (0.662 MeV), and Cobalt-60 (1.173 and 1.333 MeV). These radionuclides are widely utilized in medical imaging, nuclear medicine, industrial radiography, and radiation shielding research (Rogo *et al.,* 2025). Upon completion of the calculations, the resulting data were exported in Microsoft Excel format for further analysis and interpretation using Origin software.

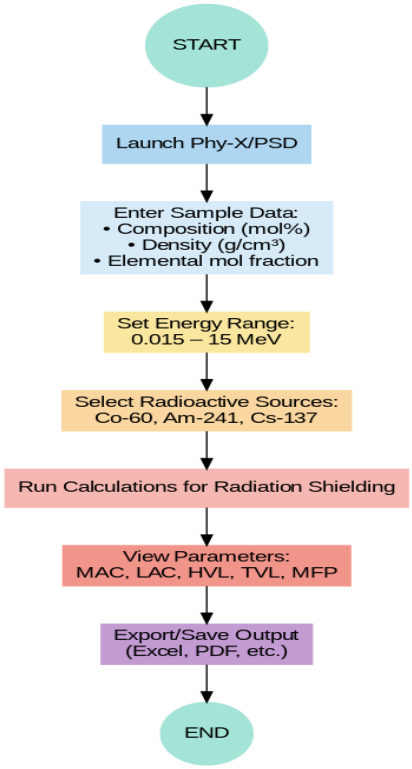

Figure 1: Methodology flowchart of using Phy-X/PSD software (Maijawa *et al*., 2025)

RESULTS AND DISCUSSION

Effective Atomic Number (Z_{eff})

The effective atomic number (Z_{eff}) is an important parameter used to describe the photon interaction capability of composite materials such as glass. The calculated Z_{eff} values for the investigated borotellurite glass samples at photon energies corresponding to commonly used radioactive sources are presented in Table 2.

Table 2: Calculated Effective Atomic Number of the Glass Sample using Phy-X

Glass Code	Gamma Radiation Sources (MeV)			
	Am-241 (0.06)	Cs-137 (0.662)	Co-60 (1.173)	Co-60 (1.333)
S1	44.99237	11.23351	10.83062	10.80730
S2	51.01006	14.47978	13.29439	13.20441
S3	55.45693	17.60090	15.71828	15.56723
S4	58.87702	20.60399	18.10324	17.89649
S5	61.58915	23.49560	20.45022	20.19292

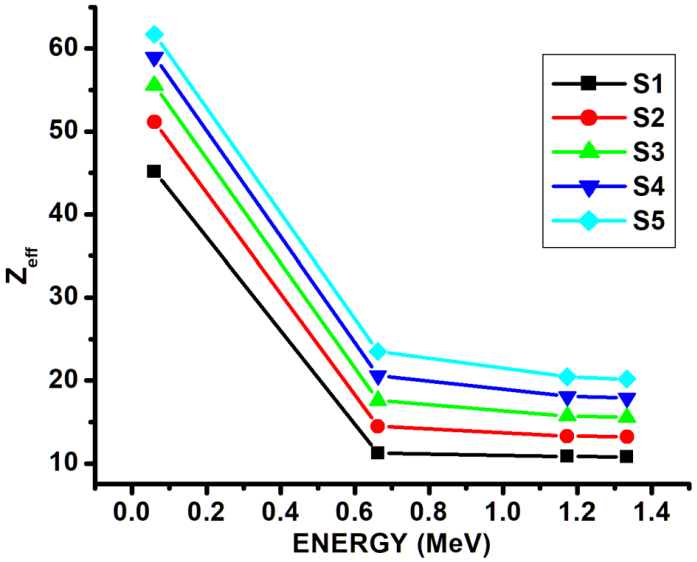

Figure 2: The Z_{eff} of the glass samples

From Figure 2, it was observed that, the Z_{eff} increases systematically with increasing Bi_2O_3 concentration in the glass matrix. At low photon energy (0.060 MeV), corresponding to the gamma emission from Americium-241, the Z_{eff} values increase significantly from 44.99 for sample S1 to 61.59 for sample S5. This strong increase can be attributed to the dominance of the photoelectric absorption process, which exhibits a strong dependence on the atomic number of the absorbing material. Since the photoelectric cross section is approximately proportional to Z^{4-5}, the incorporation of the high atomic number element bismuth (Z is 83) greatly enhances photon absorption at low energies (Abdelghany *et al.,* 2022). At intermediate photon energy (0.662 MeV), corresponding to the emission energy of Cesium-137, the Z_{eff} values decrease compared to those at lower energy but still exhibit an increasing trend with Bi_2O_3 concentration. The values increase from 11.23 (S1) to 23.49 (S5), indicating improved photon interaction probability as the Bi_2O_3 content increases. In this energy region, the Compton scattering mechanism becomes the dominant interaction process, which depends mainly on the electron density of the material rather than strongly on the atomic number. At higher photon energies of 1.173 MeV and 1.333 MeV, corresponding to the gamma emissions of Cobalt-60, the Z_{eff} values show a slight decrease relative to the intermediate energy region but continue to increase with Bi_2O_3 incorporation. In this high-energy region, pair production becomes a significant interaction mechanism, particularly above the threshold energy of 1.022 MeV. Although pair production also depends on the atomic number of the absorber, its dependence is weaker compared with the photoelectric effect (Bawazeer *et al.,* 2023). Overall, the results demonstrate that increasing the concentration of Bi_2O_3 significantly enhances the effective atomic number of the glass system across all investigated photon energies. Among the studied compositions, sample S5 containing 0.20 mol % Bi_2O_3 consistently exhibited the highest Z_{eff} values, confirming its superior radiation attenuation capability. At a similar

photon energy of 1.173 MeV, the S5 glass sample had a Z_{eff} of 20.45, which is higher than the 18.51 reported by (Rusni et al., 2024). These findings are consistent with previous studies on heavy metal oxide glasses, where the incorporation of high-Z elements such as bismuth oxide has been shown to improve gamma-ray shielding performance.

The Effective Electron Density (N_{eff})

The effective electron density (N_{eff}) provides important insight into the number of electrons available for photon interactions in the material. The calculated N_{eff} values for the investigated glass samples at selected photon energies are presented in Table 3 and illustrated in Figure 3.

Table 3: Calculated Effective Electron Density of the Glass Sample using Phy-X

Glass Code	Gamma Radiation Sources (MeV)			
	Am-241 (0.06)	Cs-137 (0.662)	Co-60 (1.173)	Co-60 (1.333)
S1	1.17×10^{24}	2.91×10^{23}	2.80×10^{23}	2.80×10^{23}
S2	1.10×10^{24}	3.10×10^{23}	2.85×10^{23}	2.83×10^{23}
S3	1.02×10^{24}	3.22×10^{23}	2.87×10^{23}	2.85×10^{23}
S4	9.40×10^{23}	3.29×10^{23}	2.89×10^{23}	2.85×10^{23}
S5	8.72×10^{23}	3.32×10^{23}	2.89×10^{23}	2.85×10^{23}

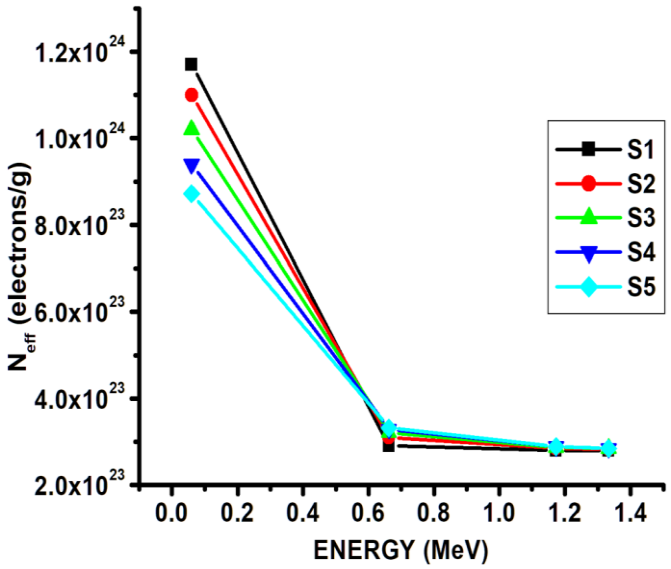

Figure 3: The N_{eff} of the glass samples

As shown in Figure 3, the effective electron density of the glass samples is strongly dependent on the energy of the gamma photons. At 0.060 MeV, the N_{eff} effective electron density exhibits an unexpected trend. As the Bi_2O_3 concentration increases from S1 to S5, the effective electron density decreases significantly. For instance, the value for sample S1 (1.17×10^{23} electrons/g) is considerably higher than for sample S5 (8.72×10^{23} electrons/g). This finding is counter-intuitive, as one would generally expect a high-Z material like bismuth (Z is 83) to enhance shielding properties at low energies where the photoelectric effect is dominant. This result suggests that the specific energy of the 0.060 MeV source may interact with a complex superposition of photoelectric absorption edges of the constituent elements (boron, tellurium, and bismuth) in a way that is not a simple linear function of concentration. At higher energy sources such as Cs-137 (0.662 MeV) and Co-60 (1.173 MeV, 1.333 MeV), the trend is reversed and more predictable. As the concentration of Bi_2O_3 increases, the effective electron density also increases. For the Cs-137 source, the value rises from 2.91×10^{23} electrons/g for S1 to 3.32×10^{23} electrons/g for S5. A similar, though less pronounced, increase is observed for the Co-60 sources. This behavior is consistent with the higher density and greater electron population of the Bi_2O_3-rich samples, which directly influences the dominant gamma-ray attenuation mechanisms in these energy ranges.

The Effective Conductivity (C_{eff})

The calculated effective conductivity (C_{eff}) values for the glass samples are presented in Table 4 and illustrated in Figure 4. The results indicate that C_{eff} strongly depends on both photon energy and Bi_2O_3 concentration.

Table 4: Calculated Effective Conductivity (S/m) of the Glass Sample using Phy-X

Glass Code	Gamma Radiation Sources (MeV)			
	Am-241 (0.06)	Cs-137 (0.662)	Co-60 (1.173)	Co-60 (1.333)
S1	4.29×10^9	1.07×10^9	1.03×10^9	1.03×10^9
S2	4.66×10^9	1.32×10^9	1.22×10^9	1.21×10^9
S3	4.61×10^9	1.46×10^9	1.31×10^9	1.29×10^9
S4	4.62×10^9	1.62×10^9	1.42×10^9	1.40×10^9
S5	4.53×10^9	1.73×10^9	1.50×10^9	1.48×10^9

As illustrated in Figure 4, a sharp decrease in conductivity is observed as the energy increases from 0.06 MeV to 0.662 MeV. This is followed by a slight, gradual decrease in conductivity at higher energies, specifically between 1.173 MeV and 1.333 MeV. At lower energy (0.060 MeV), the glasses recorded the highest effective conductivity, with values ranging from 4.29 × 10^9 S/m (S1) to 4.66 × 10^9 S/m (S2). This enhanced conductivity at low energies is due to the dominance of the photoelectric effect, which strongly depends on both the atomic number and the density of the absorber. As photon energy increased to the intermediate and high-energy regions (0.662–1.333 MeV), C_{eff} values dropped significantly. For instance, at 1.333 MeV, C_{eff} decreased to 1.03 × 10^9 S/m for (S1) and 1.48 × 10^9 S/m for (S5). A similar trend is observed across all other samples, with the most significant drop occurring in the low- to mid-energy range.[4]This reduction is associated with the shift in the dominant interaction mechanism from the photoelectric effect to Compton scattering and, at higher energies, pair production, which exhibit weaker dependence on Z. Although sample S2 exhibits slightly higher effective conductivity at the lowest photon energy (0.060 MeV), sample S5 demonstrates superior and more consistent shielding performance across the entire investigated energy range, making it the most effective overall composition.

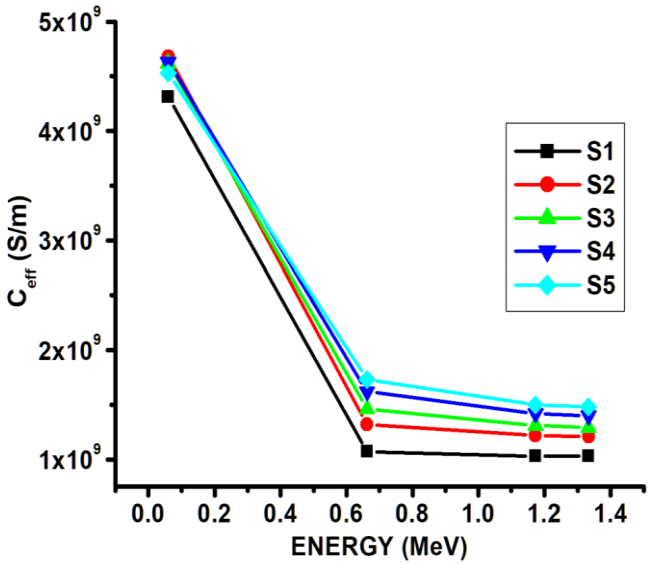

Figure 4: The C_{eff} of the glass samples

Figure 4 indicate a clear positive correlation between Bi_2O_3 concentration and effective conductivity (C_{eff}) at all investigated energies. Glass sample S5, containing the highest Bi_2O_3 content (0.2 mol %), consistently displayed the greatest shielding efficiency, with C_{eff} values of 4.53 × 10^9 S/m (0.060 MeV) and 1.48 × 10^9 S/m (1.333 MeV). This improvement can be attributed to the high atomic number (Z is 83) and density of Bi_2O_3, which enhance the probability of photon interactions, especially through the photoelectric effect. The incremental increase in C_{eff} across S1–S5 also confirms that Bi_2O_3 acts as an efficient radiation shielding modifier within the borotellurite network. Notably, the improvement in shielding performance was more pronounced at low and intermediate photon energies, where heavy-metal oxides such as Bi_2O_3 are most effective. At higher energies (above 1 MeV), although the effect of Bi_2O_3 remains evident, the relative increase in C_{eff} is less significant due to the dominance of interaction mechanisms that are less sensitive to Z.

CONCLUSION

In this work, the gamma-ray shielding characteristics of Bi_2O_3-modified thulium-doped borotellurite glasses were evaluated using the computational platform Phy-X/PSD over a wide photon energy range. The results demonstrated that the incorporation of Bi_2O_3 significantly improves the shielding performance of the glass system due to the high atomic number and density of bismuth oxide. The effective atomic number (Z_{eff}) showed a clear increase with increasing Bi_2O_3 concentration across all photon energies, indicating enhanced photon interaction probability. The effective electron density (N_{eff}) exhibited energy-dependent behavior, with a decrease at low photon energy followed by an increasing trend at higher energies as the Bi_2O_3 content increased. Additionally, the effective conductivity (C_{eff}) values were found to be highest at low photon energies due to the dominance of the photoelectric absorption mechanism, while a gradual decrease was observed at higher energies where Compton scattering and pair production dominate. Among the studied samples, the glass containing 0.2 mol % Bi_2O_3 (S5) demonstrated the best overall radiation shielding capability. These results confirm that Bi_2O_3 incorporation effectively enhances the radiation attenuation properties of borotellurite glasses, making them promising lead-free shielding materials for applications in medical imaging facilities, nuclear laboratories, and other radiation protection environments. Future work may include experimental validation and neutron shielding assessment to further confirm the practical applicability of these glasses.

REFERENCES

Abdelghany, Y. A., Kassab, M. M., Radwan, M. M., & Abdel-Latif, M. A. (2022). Borotellurite glass system doped with ZrO2, potential use for radiation shielding. Progress in Nuclear Energy, 149, 104256. https://doi.org/10.1016/j.pnucene.2022.104256

AbuAlRoos, N. J., Baharul Amin, N. A., & Zainon, R. (2019). Conventional and new lead-free radiation shielding materials for radiation protection in nuclear medicine: A review. Radiation Physics and Chemistry, 165, 108439. https://doi.org/10.1016/j.radphyschem.2019.108439

Alomari, A. H. (2024). Enhancing radiation shielding effectiveness: A comparative study of barium-doped tellurite glasses for gamma and neutron radiation protection. Journal of Taibah University for Science, 18(1), 2328370. https://doi.org/10.1080/16583655.2024.2328370

Alothman, M. A., Alrowaili, Z. A., Alzahrani, J. S., Wahab, E. A. A., Olarinoye, I. O., Sriwunkum, C., Shaaban, Kh. S., & Al-Buriahi, M. S. (2021). Significant influence of MoO3 content on synthesis, mechanical, and radiation shielding properties of B2O3-Pb3O4-Al2O3 glasses. Journal of Alloys and Compounds, 882, 160625. https://doi.org/10.1016/j.jallcom.2021.160625

Azuraida, A., Nurshahidah, O., Yusoff, W. Y. W., Falihan, R., Abdul-Manaf, N. A., & Ahmad, N. (2022). Effect of thulium boro-tellurite glass system on radiation shielding parameters. Journal of Ovonic Research, 18(2), 141–148. https://doi.org/10.15251/JOR.2022.182.141

Barbhuiya, S., Das, B. B., Norman, P., & Qureshi, T. (2025). A comprehensive review of radiation shielding concrete: Properties, design, evaluation, and applications. Structural Concrete, 26(2), 1809–1855. https://doi.org/10.1002/suco.202400519

Bawazeer, O., Makkawi, K., Aga, Z. B., Albakri, H., Assiri, N., Althagafy, K., & Ajlouni, A.-W. (2023). A review on using nanocomposites as shielding materials against ionizing radiation. Journal of Umm Al-Qura University for Applied Sciences, 9(3), 325–340. https://doi.org/10.1007/s43994-023-00042-9

Devillers, M. A. C. (1984). Lifetime of electrons in metals at room temperature. Solid State Communications, 49, 1019–1022. https://doi.org/10.1016/0038-1098(84)90413-7

Frane, N., & Bitterman, A. (2025). Radiation Safety and Protection. In StatPearls. StatPearls Publishing. http://www.ncbi.nlm.nih.gov/books/NBK557499/

Hussain, S., Mubeen, I., Ullah, N., Shah, S. S. U. D., Khan, B. A., Zahoor, M., Ullah, R., Khan, F. A., & Sultan, M. A. (2022). Modern Diagnostic Imaging Technique Applications and Risk Factors in the Medical Field: A Review. BioMed Research International, 2022, 5164970. https://doi.org/10.1155/2022/5164970

Ibrahim, S., Ali, A. A., & Fathi, A. M. (2024). A comprehensive investigation of Bi2O3 on the physical, structural, optical, and electrical properties of K2O.ZnO.V2O5.B2O3 glasses. Scientific Reports, 14(1), 8518. https://doi.org/10.1038/s41598-024-58567-w

Kamislioglu, M. (2021). An investigation into gamma radiation shielding parameters of the (Al:Si) and (Al+Na):Si-doped international simple glasses (ISG) used in nuclear waste management, deploying Phy-X/PSD and SRIM software. Journal of Materials Science: Materials in Electronics, 32(9), 12690–12704. https://doi.org/10.1007/s10854-021-05904-8

Kaur, A. S., Khanna, A., & Gonzalez, F. (2016). Structural, optical, dielectric and thermal properties of molybdenum tellurite and borotellurite glasses | Request PDF. ResearchGate. https://doi.org/10.1016/j.jnoncryso1.2016.04.033

Kaur, P., Singh, D., & Singh, T. (2016). Heavy metal oxide glasses as gamma rays shielding material. Nuclear Engineering and Design, 307, 364–376. https://doi.org/10.1016/j.nucengdes.2016.07.029

Laxmikanth, C., Elias, A. M., Sichone, S., & Mwankemwa, B. (2025). Tailoring structural, thermal, and optical properties of Tm3+-doped borotellurite glasses through Bi2O3 incorporation for optical fiber construction. Next Materials, 6, 100274. https://doi.org/10.1016/j.nxmate.2024.100274

Maijawa, I., Musa, A., & Rogo, H. S. (2025). Investigation of the Impact of Bi2O3 Addition on the Radiation Shielding Performance of Tm3+-Doped Borotellurite Glasses Via the Phy-X/PSD Software. Nexus of Future Materials, 2, 239–244. https://doi.org/10.70128/632030

Marzuki, A., Suryana, R., Syamsyiah, N., Fausta, D. E., Kabalci, I., & Rodliyatul Jauhariyah, M. N. (2025). Optical, structural, and gamma radiation shielding properties of lead borate glasses containing a small fraction of crystalline phase. Radiation Physics and Chemistry, 233, 112712. https://doi.org/10.1016/j.radphyschem.2025.112712

Munakata, Y., Sato, Y., Maki, T., Sekine, K., Sakai, Y., Oishi, K., & Torii, K. (2009). Study on Radiation Shielding Performance of Reinforced Concrete Wall (2): Shielding Analysis.

Naja, G. M., & Volesky, B. (2017). Toxicity and Sources of Pb, Cd, Hg, Cr, As, and Radionuclides in the Environment. In Handbook of Advanced Industrial and Hazardous Wastes Management (pp. 855–903). CRC Press.

Raj, K., & Das, A. P. (2023). Lead pollution: Impact on environment and human health and approach for a sustainable solution. Environmental Chemistry and Ecotoxicology, 5, 79–85. https://doi.org/10.1016/j.enceco.2023.02.001

Rogo, H. S., Musa, A., & Maijawa, I. (2025). Investigation of gamma-ray shielding performance of borosilicate glasses doped with TiO2 using Phy-x/PSD and Xcom software. Fudma Journal of Sciences, 9(6), 64–72. https://doi.org/10.33003/fjs-2025-0906-3484

Rusni, N. A. M., Laoding, H., & Amat, A. (2024). Theoretical Ionizing Radiation Shielding Parameters of Thulium Doped Zinc Borotellurite Glass. E3S Web of Conferences, 481, 03009. https://doi.org/10.1051/e3sconf/202448103009

Şakar, E., Özpolat, Ö. F., Alım, B., Sayyed, M. I., & Kurudirek, M. (2020). Phy-X / PSD: Development of a user friendly online software for calculation of parameters relevant to radiation shielding and dosimetry. Radiation Physics and Chemistry, 166, 108496. https://doi.org/10.1016/j.radphyschem.2019.108496

Sayyed, M. I., Mohammed, F. Q., Mahmoud, K. A., Lacomme, E., Kaky, K. M., Khandaker, M. U., & Faruque, M. R. I. (2020). Evaluation of Radiation Shielding Features of Co and Ni-Based Superalloys Using MCNP-5 Code: Potential Use in Nuclear Safety. Applied Sciences, 10(21), 7680. https://doi.org/10.3390/app10217680

Wang, Y., Ding, P., Xu, H., Li, Q., Guo, J., Liao, X., & Shi, B. (2020). Advanced X-ray Shielding Materials Enabled by the Coordination of Well-Dispersed High Atomic Number Elements in Natural Leather. ACS Applied Materials & Interfaces, 12(17), 19916–19926. https://doi.org/10.1021/acsami.0c01663

Yin, S., Wang, H., Li, A., Ma, Z., & He, Y. (2022). Study on Radiation Shielding Properties of New Barium-Doped Zinc Tellurite Glass. Materials, 15(6), 2117. https://doi.org/10.3390/ma15062117